PHOTOEFFECTS IN METAL-Zn_3P_2 CONTACTS*. PART I. A MODEL

By K. Nauka and J. M. Pawlikowski

Institute of Physics, Technical University of Wrocław**

(Received June 13, 1980)

A simple model for the analysis of photo-carrier distributions and photo-voltage generations for the metal-semiconductor contact is presented. This model takes into account the optical absorption of the semiconductor and metal contact as well as carrier recombination effects in the volume and on the surfaces. Carrier-distribution equations are solved and hence the photo-responses are computed for the metal-Zn_3P_2 Schottky barrier. A comparison of the computed results and experimental data for the Au-Zn_3P_2 structure yields sufficiently good agreement.

PACS numbers: 72.40.+w, 73.40.Ns

1. Introduction

Recently, there has been great interest in the use of metal-semiconductor structures as solar cells. This interest is mainly supported by their simplicity and low cost of production — they may be formed at low temperatures and by relatively simple technological methods.

The optimal energy gap (Eg) values of the semiconductor used, under both outer space (AMO) and terrestrial (AM2) conditions is close to 1.45 eV, [1]. From this viewpoint, Zn_3P_2 is a very promising semiconductor [2, 3], having an energy gap of 1.5 eV at 300 K [4].

The aim of this paper is to give a simple theoretical model of the photo-effects on the metal-Zn_3P_2 Schottky junction. A comparison of calculated results and experimental data is finally presented and shows sufficiently good consistency.

2. A model of photovoltage (PV) effect

The fundamental semiconducting properties of Zn_3P_2 are presented in [5], and the spectral dependences of the absorption coefficient, α, at several temperatures, is taken from [4]. Trapping levels located within an energy gap of Zn_3P_2 heve been not found

* Work sponsored under contract IM-132.

** Address: Instytut Fizyki, Politechnika Wrocławska, St. Wyspiańskiego 27, 50-370 Wrocław, Poland.

experimentally so far [6], so the bipolar photo-carrier generations will be considered. The standard configuration of metal electrodes is assumed, as in the Schottky-barrier solar cells [7]. In such a configuration, the region of the semiconductor near the barrier contact is of most importance; therefore, the photo-carrier distributions will be calculated for this region only. The thickness of the metal (contact) layer is assumed to be 10 nm. Two regions in the semiconductor will be taken into account: (*i*) the bulk region where photo-carrier distributions are determined by the ambipolar diffusion only, and (*ii*) depletion region (near the barrier contact) where the potential barrier appears besides the Dember field. Let us assume a low photon flux density, then the conditions of low excitations ($\Delta n \ll n_0$ and $\Delta p \ll p_0$) are satisfied ($n_0, p_0, \Delta n$ and Δp denote the "dark" and excess concentrations of electrons and holes, respectively). So, the generated carriers do not affect the band bending, and the barrier field is only determined by the acceptor density. In this case the barrier-field shape is given by the well-known formula (for $t_s \geqslant x \geqslant t_b$):

$$E_b(x) = \phi_B \frac{x-t_b}{t_d} \tag{1}$$

where ϕ_B is a barrier height, t_b and t_d are the thicknesses of the bulk and depletion regions, respectively. For the one-dimensional photon flux (monochromatic irradiance of the sam-

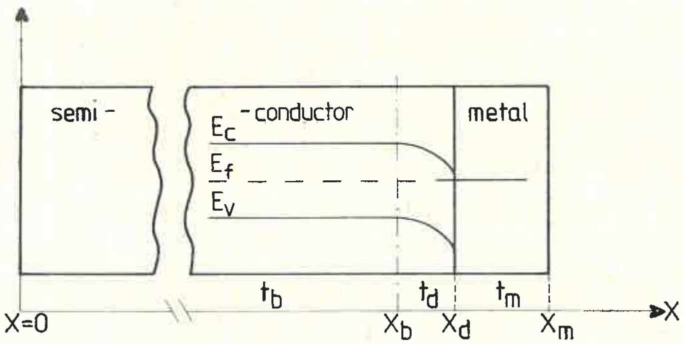

Fig. 1. Configuration of the structure considered. Semiconductor thickness is $t_s = t_b + t_d$

ple in the x-axis direction is taken), the one-dimensional model of photo-carrier distributions can be taken into account. Since the minority carriers effectively determine the PV-effect, the discussion will be restricted to the excess-electron distribution. The schematic configuration of structure considered is shown in Fig. 1.

3. *The distribution equations*

The well-known form of the distribution equation (under isothermic conditions and without a magnetic field) is as follows (see e.g. [8]):

$$\frac{d^2}{dx^2}\Delta n + \kappa E \frac{d}{dx}\Delta n + \kappa\left(\frac{d}{dx}E - \frac{1}{\mu_e \tau_e}\right)\Delta n + \frac{G(x)}{D_e} = 0, \tag{2}$$

where E is the x-component of an electric field of arbitrary origin (external and/or internal), τ_e is an excess-electron life-time, D_e is an electron diffusion constant given by the well-known Einstein relation and $\kappa = e/kT$. For monochromatic radiation, the photo-carrier generation rate, G, is given by

$$G(x) = I_0\alpha \exp(-\alpha x), \tag{3}$$

where I_0 is the photon flux per unit time and per unit front area, and α is the absorption coefficient of the semiconductor. Considering two parts of specimen, Eq. (2) has to be solved for each part separately.

3.1. Bulk region

In this region, the electron distribution is determined by the Dember field only. So one can describe Eq. (2) in the form

$$\frac{d^2}{dx^2}\Delta n - \frac{1}{D_a\tau_e}\Delta n + \frac{G(x)}{D_a}, \tag{4}$$

where D_a is an ambipolar diffusion constant

$$D_a = D_e\frac{n+p}{bn+p} = bD_h\frac{n+p}{bn+p} \tag{5}$$

($n = n_0+\Delta n$, $p = p_0+\Delta p$), which tends to D_e if $p_0 \gg n_0$ and $p_0 \gg bn_0$, $b = \mu_e/\mu_h$. The solution of Eq. (4) has the form

$$\Delta n(x) = A_1 \exp\left(\frac{x}{L_1}\right) + B_1 \exp\left(-\frac{x}{L_1}\right) + C_1 \exp(-\alpha x), \tag{6}$$

where

$$C_1 = \frac{\alpha I_0 \tau_e}{1-\alpha^2 L_1^2}, \tag{7}$$

$L_1 = (D_a\tau_e)^{1/2}$ is a difussion length, and A_1 and B_1 are easily expressed by the boundary conditions (see e.g. [8]). In this case, the surface recombination rates will be assumed as $S_1\,(x = 0) = S_2(x = x_b) = 0$, to clarify the calculations. This is justified, on the one hand, by the lack of a real boundary at x_b and, on the other, by the fact that the excess-carrier concentrations far away the barrier contact do not have the essential meaning.

3.2. Depletion region

A thickness of the depletion region, in the simplest model of the Schottky barrier [9], is given by the formula

$$t_d = \frac{2\varepsilon_0\varepsilon_s\phi_B}{eN_A} \tag{8}$$

with an accuracy up to several lattice constants. The distribution equation in this region is

$$\frac{d^2}{dx^2}\Delta n + \kappa[E_b(x)+E_D(x)]\frac{d}{dx}\Delta n + \kappa\left\{\frac{d}{dx}[E_b(x)+E_D(x)] - \frac{1}{\mu_e\tau_e}\right\}\Delta n + \frac{G(x)}{D_e} = 0. \tag{9}$$

Usually, the Dember field (of the order of kT/e) is less than the barrier field (of the order of 1 eV); hence, the former can be neglected in the first approximation. However, such an equation may be solved approximately only [10]. Two boundary conditions are used to solve Eq. (9). The first boundary condition is based on the assumption that the photo--carrier distribution is ambipolar at the point $x = x_b$, hence

$$\Delta n(x = x_b) = A_1 \exp\left(\frac{x_b}{L_1}\right) + B_1 \exp\left(-\frac{x_b}{L_1}\right) + C_1(-\alpha x_b). \tag{10}$$

The second boundary condition includes the front-surface recombination and the current of carriers (holes in this case) photo-emitted from the metal to the semiconductor, j_m. Thus, we have

$$j_e = eS_1 \Delta n(x = x_d) + j_m, \tag{11}$$

where

$$j_e = eD_e \left.\frac{d(\Delta n)}{dx}\right|_{x=x_d} + e\mu_e \Delta n E_b(x = x_d).$$

The density of j_m is taken from the Fowler theory [11] modified in [12, 13].

The solution of Eq. (9) has the form of an exponential series

$$\Delta n(x) = \sum_{\nu=0}^{\infty} c_\nu (x - x_d)^\nu. \tag{12}$$

Some initial terms (strongly decreasing, fortunately, due to the small values of $x - x_d$) have coefficients as follows:

$$c_0 = \Delta n(x_d),$$

$$c_1 = \left\{\Delta n(x_d) - \Delta n(x_b) + \frac{\alpha I_0}{D_e}\frac{t_d^2}{2}\exp(-\alpha x_d)\left[1 + \frac{t_d}{3}\left(\alpha + \frac{e\phi_B}{kT}\left(\frac{e\phi_B}{kTt_d} - \frac{t_d}{D_e\tau_e}\right)\right)\right.\right.$$
$$\left.\left. + \frac{\alpha^2 t_d^2}{6} + \frac{\alpha^3 t_d^3}{10}\right]\right\}\left\{t_d + \frac{t_d^2}{2}\frac{e\phi_B}{kT}\left(\frac{e\phi_B}{kTt_d} - \frac{t_d}{D_e\tau_e}\right) + \frac{t_d^3}{6}\left[\frac{e\phi_B}{kT}\left(\frac{e\phi_B}{kTt_d} - \frac{t_d}{D_e\tau_e}\right)\right]^2\right\}^{-1},$$

$$c_2 = \tfrac{1}{2}\left[\frac{\alpha I_0}{D_e}\exp(-\alpha x_d) - C_1\frac{e\phi_B}{kT}\left(\frac{e\phi_B}{kTt_d} - \frac{t_d}{D_e\tau_e}\right)\right],$$

$$c_3 = \tfrac{1}{6}\left\{-\alpha c_2 - \frac{e\phi_B}{kT}\left(\frac{e\phi_B}{kTt_d} - \frac{t_d}{D_e\tau_e}\right)c_2 + \left[\frac{e\phi_B}{kT}\left(\frac{e\phi_B}{kTt_d} - \frac{t_d}{D_e\tau_e}\right)\right]^2\right\},$$

$$c_4 = \tfrac{1}{12}\frac{\alpha^3 I_0}{D_e}\exp(-\alpha x_d),$$

$$c_5 = -\tfrac{1}{20}\frac{\alpha^4 I_0}{D_e}\exp(-\alpha x_d),$$

$$c_6 = \tfrac{1}{30}\frac{\alpha^5 I_0}{D_e}\exp(-\alpha x_d), \ldots \tag{13}$$

4. Discussion and conclusions

The computational results of photo-carrier distributions are presented in Figs. 2–4, as the $\Delta n(x)$ plots for two different lighting configurations. The distribution curves for the back-wall configuration are presented in Fig. 2, for a relatively thick semiconductor. Plots for three wavelength values are shown, as an example[1]. The strong decrease of $\Delta n(x)$

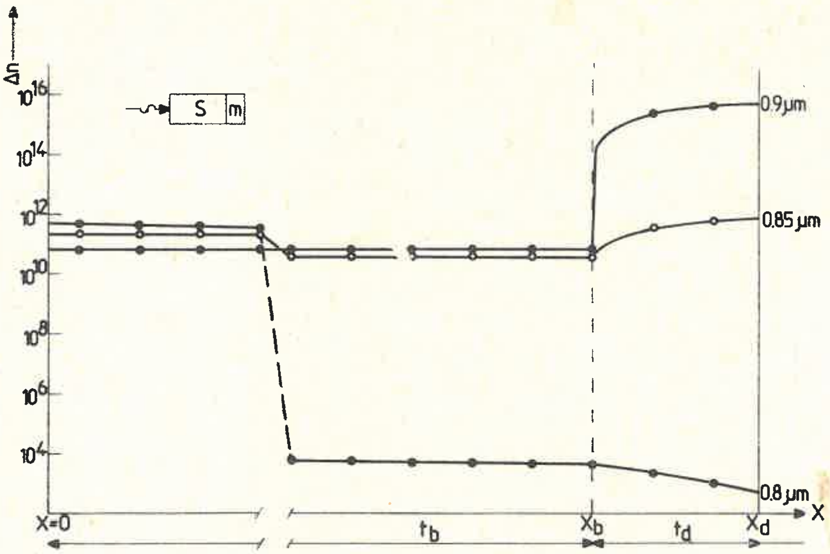

Fig. 2. $\Delta n(x)$ plots (in arbitrary units) for the back-wall lighting configuration. Exemplary wavelengths are shown, and indicated in the figure. The bulk-semiconductor thickness is assumed as $t_b = 20\,L_1$. The fitting parameter is the photon flux density I_0

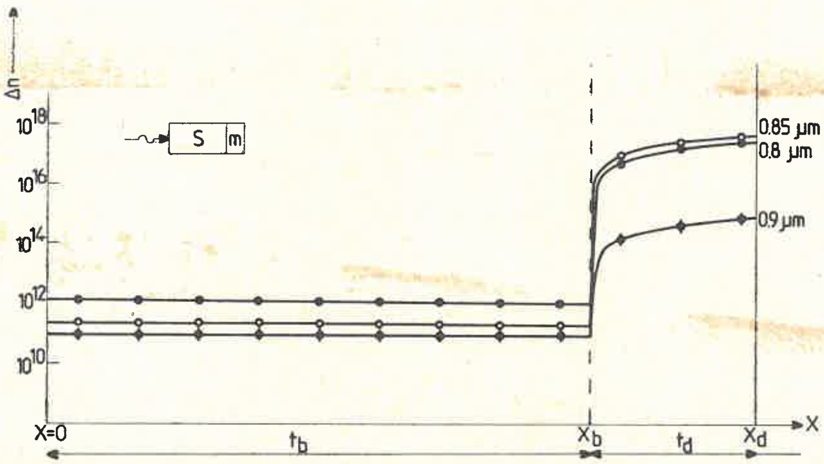

Fig. 3. $\Delta n(x)$ plots as in Fig. 2. but for the thin bulk region, $t_b = L_1$

[1] They were chosen to satisfy the condition $E_g^i \lesssim \hbar\omega_1 < \hbar\omega_2 \lesssim E_g^d \lesssim \hbar\omega_3$, where E_g^i and E_g^d denote the indirect and direct energy gap at 300 K [4].

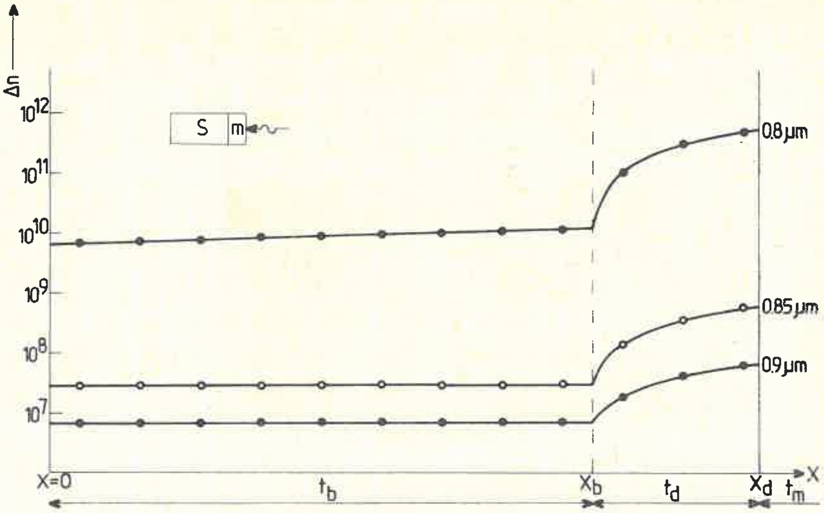

Fig. 4. $\Delta n(x)$ plots for the front-wall lighting configuration. The thickness of the semi-transparent metal layer, t_m, is equal to 10 nm

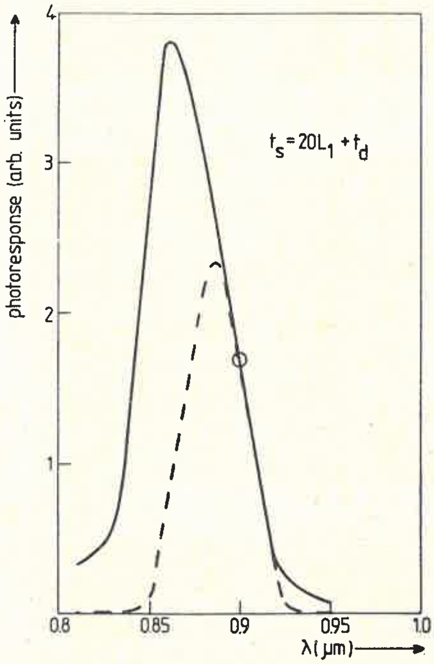

Fig. 5. A comparison of experimental (solid line) and theoretical (broken line) photoresponses for the back-wall configuration and for the thick bulk region of the semiconductor. A fit is made at the point indicated, by the chosen value of I_0

was observable for $\lambda \leqslant 0.8$ μm, both in the bulk and depleted region, due to high absorption. $\Delta n(x)$ plots rise in the depletion region for photons with smaller energies. This is evident due to an effect of the barrier field. The same effect is obviously seen for all the wavelengths in the case of a thin semiconductor and under the same lighting configuration, shown in Fig. 3. However, no drop in the bulk region is stated and a rise of $\Delta n(x)$ in the depleted region is greater than for thicker specimens. A comparison of plots in Fig. 2 and Fig. 3 shows the essential meaning of photon density reaching a region near the metal--semiconductor interface. There must be a balance between the values of the absorption coefficient and semiconductor thickness.

In contrast, the plots under front-wall irradiance are shown in Fig. 4. A semi-transparent metal layer of 10 nm thick was assumed in the computations. The absorption coefficient of the metal is independent of the wavelengths for the values considered. Hence, the greatest values of $\Delta n(x)$ are found for photons with the greatest energies (i.e. for the strongest absorption). However, the total values of $\Delta n(x)$ are smaller in this case, in contrast to the irradiance configuration discussed above. This is due to absorption by a metal contact.

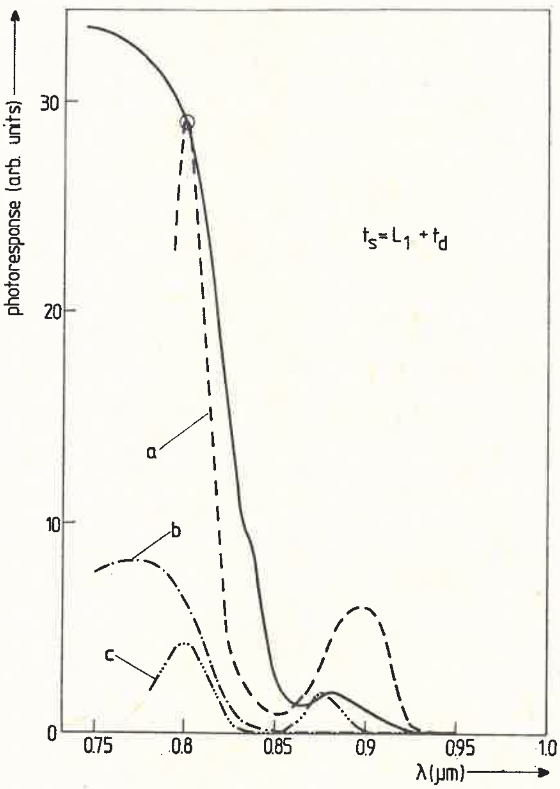

Fig. 6. Experimental plot (solid line) for the front-wall configuration compared with the theoretical one *a*) under back-wall lighting, but for a thin semiconductor. A fit is made at the point indicated. Curves *b*) and *c*) are computed for the front-wall configuration, for 10 nm thick metal *b*) and for the 5 nm thick one *c*)

On the basis of computations (examples are presented in Figs. 2–4) the total concentrations of excess electrons, ΔN, were computed as

$$\Delta N = \int_{x_1}^{x_2} dx \Delta n(x), \tag{14}$$

where $x_1 = 0$ or $x_1 = x_b - L_1$ (for a thin or thick semiconductor, respectively) and $x_2 = x_b$, for the bulk region, and $x_1 = x_b$ and $x_2 = x_d$, for the depletion region. Having known the spectral dependences of the Zn_3P_2 absorption coefficient [4], we have computed the spectral responses of the Au—Zn_3P_2 Schottky junction, presented in Figs. 5 and 6. Also shown in these figures are the experimental curves (solid lines) obtained from investigations of the Au—Zn_3P_2 structure published recently [14].

The theoretical curve, presented in Fig. 5 satisfies the condition of the back-wall illumination through the relatively thick semiconductor [14]. As it is shown, a sufficiently good accordance appears, particularly for the long-wave threshold, characterising the indirect optical transitions in the Zn_3P_2 band structure [4].

The experimental curve in Fig. 6 shows a photoresponse of the structure under front-wall irradiance, through a semi-transparent metal layer [14]. The theoretical curve *a* was calculated for the case of back-wall illumination, but through the thin semiconductor which is the case equivalent to front-wall irradiation near the contact, as for the experimental plot. Curves *b* and *c* were computed (also for a thin semiconductor) for the case of front-wall illumination, for the relatively thin metal layer ($t_m = 5$ nm) — curve *c*, and for the thicker one ($t_m = 10$ nm) — curve *b*. For a thick metal layer, the indirect-transition response disappears; whereas, for the thinner one, the indirect band-to-band excitation also makes the photo-response, as it is visible in experiments. There is the qualitative accordance between the theoretical and experimental long-wave thresholds, for direct optical transitions in the Zn_3P_2 band structure.

In conclusion, we can note that our simple model qualitatively describes the experimentally observed photoresponses, with sufficient consistency.

We express our thanks to Miss N. Mirowska for the experimental data facilities and to Dr J. Misiewicz for discussing of Zn_3P_2 absorption spectra with us.

REFERENCES

[1] J. J. Loferski, *J. Appl. Phys.* **27**, 777 (1956), and H. J. Hovel, *Semiconductor and Semimetals*, ed. Willardson and Beer, Acad. Press N. Y., vol. 11 (1975).
[2] J. M. Pawlikowski, N. Mirowska, F. Królicki, *Infrared Phys.* **18**, 343 (1978).
[3] N. Convers Wyeth, A. Catalano, *J. Appl. Phys.* **50**, 1403 (1979).
[4] J. M. Pawlikowski, J. Misiewicz, N. Mirowska, *J. Phys. Chem. Solids* **40**, 1027 (1979).
[5] W. Żdanowicz, *Postępy Fiz.* **26**, 613 (1975).
[6] K. Nauka, Reports of T.U.W., I-9/80, unpublished.
[7] R. F. McOuat, D. L. Pulfrey, *J. Appl. Phys.* **47**, 2113 (1976).
[8] J. M. Pawlikowski, *Mater. Sci.* **6**, 3 (1980) and *Infrared Phys.* **20**, 257 (1980).

[9] S. M. Sze, *Physics of Semiconductor Devices*, ed. Wiley and Sons, N. Y. 1969.
[10] A. Erdelyi, *Ann. Phys.* **415**, 21 (1935).
[11] R. H. Fowler, *Phys. Rev.* **38**, 45 (1931).
[12] M. Leppihalme, T. Tuomi, *Phys. Status Solidi* (a) **33**, 125 (1976).
[13] J. M. Pawlikowski, J. Żyliński, *Optica Applicata* **7**, 127 (1977).
[14] J. M. Pawlikowski, N. Mirowska, P. Becla, F. Królicki, *Solid-State Electron.* **23**, 755 (1980).